

# PROSTATE DETECTION AND SEGMENTATION BASED ON CONVOLUTIONAL NEURAL NETWORK AND TOPOLOGICAL DERIVATIVE

Choongsang Cho<sup>1</sup>, Young Han Lee<sup>1\*</sup>, and Sangkeun Lee<sup>2 †</sup>

<sup>1</sup> Artificial Intelligence  
Research Center  
Korea Electronics Technology Institute  
Seongnam, Korea  
{ideafisher and yhlee}@keti.re.kr

<sup>2</sup> Graduate School of Advanced  
Imaging Science, Multimedia & Film  
Chung-Ang University  
Seoul, Korea  
sangkny@cau.ac.kr

## ABSTRACT

The topological derivative (TD) for shape analysis has been employed in image segmentation, and machine learning schemes based on convolutional neural network (CNN) provide the high performance in the image processing. The supervised and unsupervised approaches have different roles and advantages according to their concepts. To maximize the benefits of two approaches, we propose CNN-TD based segmentation approach. A CNN-based segmentation scheme is employed to faithfully consider the characteristics of an object to be segmented in a given image, and we refine the CNN results using a TD-based scheme. Experimental results show that the proposed scheme produces better performance for the prostate segmentation than the refined results by level set-based schemes. Therefore, we believe that the proposed scheme can be a useful tool for effective medical image segmentation.

**Index Terms**— Prostate Segmentation, Convolutional Neural Network, Topological Derivative, Refinement

## 1. INTRODUCTION

Medical images, which are obtained from computed tomography (CT), magnetic resonance imaging (MRI), and positron emission tomography (PET), have necessary information for specialists to diagnose customers' health. In medical imaging research, segmentation is an essential step for disease diagnosis and estimation, cancer detection and treatment, surgical planning and monitoring, and the identification of arteries [1, 2, 3, 4]. In the unsupervised image segmentation, several approaches have been proposed with level set (LS) approaches, which are a region-based active contour (AC) [2,

3] and the topological derivative (TD) approaches [4, 5] by introducing perturbation. A bias-correction scheme suppressing the inhomogeneous characteristic and a nonparametric statistical scheme reducing the complexity were proposed [2, 3]. In particular, a low-complexity TD-based approach was proposed [4]. In the supervised medical image segmentation, machine learning schemes such as convolutional neural network (CNN), random forest, and etc. have been applied to detect the disease and organ regions [1]. Deep learning-based approaches and a superpixel-based graph cut schemes have been widely applied in the prostate segmentation [1]. The supervised and unsupervised approaches have different roles and advantages according to their applications and purposes. The unsupervised schemes are strongly influenced by the given image and the cost function, on the other hand, the supervised methods are affected by the training model and its dataset because of properties in the data driven approach. Therefore, we propose a CNN-TD based segmentation approach to faithfully apply the characteristics of segmented region and to specifically consider the characteristics of a given image.

This manuscript is organized as follows: In Section 2, proposed scheme is explained in detail. The experimental results are compared and analyzed in Section 3. Finally, in Section 4, the algorithm is summarized with some discussions.

## 2. PROPOSED METHOD

The model-based segmentation schemes provide a robust performance by designing deep-layer structure and training many data. The unsupervised approaches widely used for the medical images to find the optimal solution in the given data. A segmentation method consisting of deep-learning and unsupervised methods is proposed to robustly detect and accurately segment the lesion or organ region as shown in Fig. 1. In the proposed scheme, the target region is detected by CNN-based deep-learning, and its output is segmented into disjoint regions by the TD-based method such that the detected region is precisely refined by strongly considering the characteristic of the given image.

\*C. Cho and Y.H. Lee contributed equally to this work supported by the IT R&D program of MSIP/IITP [2017-0-00255, Autonomous digital companion development].

<sup>†</sup>(Corresponding author : email:sangkny@cau.ac.kr), and this work was partially supported by the NRF funded by the Ministry of Education, Science and Technology[NRF-2014R1A2A1A11049986].

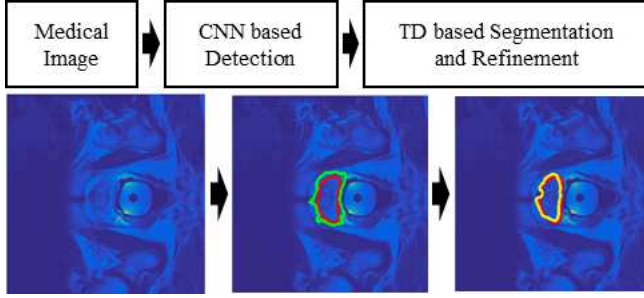


**Fig. 1.** Prostate segmentation procedure by using CNN and TD methods: red, green, and yellow lines are contours of ground truth, CNN result, and TD-based refinement result, respectively.

### 2.1. CNN-based prostate detection

In order to segment the target region from an image, end-to-end approaches have been proposed using fully convolutional or deconvolutional network [6, 7]. It is easy to access several large database opened for a research or a competition like MS COCO [8] and VOC [9]. However, in the field of medical image tasks, lack of data causes serious problems to apply the end-to-end approaches into the medical image segmentation. To overcome the problems, a patch-based image decision scheme is applied. In other words, a network determines if the given patch is a target region for all pixels with adjacent sub-image generated using a sliding window. There are two output classes in this task: prostate or not. From the data analysis of MICCAI database [10], it was investigated that the ratio between two classes is asymmetric. Only 1.94% is for the prostate class. That is, an untrained model has 98.06% accuracy by default. Therefore, the margin between the best and worst cases is too small to fit the network for this task. In order to extend the gap, database for training and validation is manipulated to increase the prostate class ratio on purpose. Specifically, non-prostate patches are randomly sampled to make the balance as much as possible. As a result, our database for training and validation has about 30% of the prostate class. However, the test dataset is not manipulated at all. From the above manipulation, the number of images in the database for training and validation is 229,183 and 98,234, respectively.

Table 1 shows the proposed convolutional neural network (CNN) architecture consisting of 4 convolutional, 2 max-pooling, and 2 FCN layers. The rectified linear unit (RELU) is used as an activation function for convolutional and FCN layers. The proposed architecture has  $1 \times 65 \times 65$  patched image as an input and 2nd order output vector to infer whether the patch is prostate region or not. A stochastic gradient decent optimization is employed with 0.01 learning rate and  $1e-6$  decaying factor. We evaluate the result with 150 epochs because the accuracy was begun to be saturated after 136th epoch on the validation.

**Table 1.** The proposed CNN-based detection network for a prostate segmentation.

Layers	Activation	Size
Convolutional (2D)	RELU	(8, 3, 3)
Convolutional (2D)	RELU	(32, 3, 3)
Max pooling		(2, 2)
Convolutional (2D)	RELU	(16, 3, 3)
Convolutional (2D)	RELU	(64, 3, 3)
Max pooling		(2, 2)
Fully connected	RELU	4469
Fully connected	Softmax	2

### 2.2. Topological derivative-based segmentation and refining the disjoint region

To segment and refine the detected region using the TD-based scheme, the minimum and maximum indexes of  $x$  and  $y$  coordinates are computed from the CNN-based result in which a region involving the prostate is obtained as

$$\begin{aligned}
 (x_{\min}, y_{\min}) &= \arg \min_{(x,y)} (L(x,y) == 1), \forall (x,y), \\
 (x_{\max}, y_{\max}) &= \arg \max_{(x,y)} (L(x,y) == 1), \forall (x,y), \\
 \text{and } v &= I(x_{\min} : x_{\max}, y_{\min} : y_{\max})
 \end{aligned} \quad (1)$$

where  $I$  and  $L$  are a given image and its label, respectively.

To segment the section  $v$  into  $N_c$  disjoint regions  $u$  by the TD-based scheme [4], the cost function  $\psi(\Omega)$  in the unperturbed domain  $\Omega$  is computed as

$$\psi(\Omega) = \frac{1}{2} \int_{\Omega} K \nabla \phi \cdot \nabla \phi d\Omega + \frac{1}{2} \int_{\Omega} [\phi - (v - u)]^2 d\Omega, \quad (2)$$

where  $K$  indicates the diffusivity tensor that is constant at image element level, and  $\phi$  is a solution of the variational problem [4].

Segmented image  $u$  consisting of  $N_c$ -th disjoint regions is obtained by iteratively computing TD based on the cost function and by finding the minimum TD among all classes. To refine the results, each region is divided into several labels by the connected component analysis.

$$u_n = \sum_{i=1}^{l_n} L(i), \text{ for } n = 1, \dots, N_c \quad (3)$$

where  $l_n$  is the number of labels in a class.

To keep the labels that have many elements close to the center position of a detected region, the elements are evaluated by the average distance from the center position of prostate region obtained CNN-based result and the pixel number of the labels as

$$Rf_i = \frac{C(L(i))}{\max(C(L))} + \left[ 1 - \frac{D_c(L(i))}{\max(D_c(L))} \right], i = 1, \dots, l_n \quad (4)$$

where  $C(\cdot)$  and  $D_c(\cdot)$  are element counting and distance measurement operators, respectively, and the distance is measured by the euclidean distance between the center position and the

pixel in the labels. Then, the evaluated region is refined by removing the labels that have smaller refinement cost  $Rf_i$  than the average cost.

### 3. EXPERIMENT

In order to evaluate the segmentation performance, the proposed scheme is compared with CNN and LS-based approaches to refine the deep-learning results for the same purpose of using TD-based scheme. The CNN-based scheme consists of 8 layers and was implemented by using Theano and Keras frameworks. For the model of CNN based deep-learning, the 45 sets in 50 prostate MRI sets [11] were used to generate the train and validation data, and the remaining sets were used for the test. To apply the CNN with limited data, the patches,  $65 \times 65$ , were extracted from the train and validation data to build the model weights. In addition, the test data was evaluated by the patches extracted from those.

The detected region by the CNN scheme is analyzed through the connected component labeling, and the CNN results are obtained after removing the small regions. For the proposed scheme, the results are refined by the TD-based or LS-based approaches. The LS-based approaches include a bias-correction-based LS scheme [2] and a nonparametric AC approach [3]. In the refinement using LS-based scheme, the region is segmented into two regions, and the region providing the highest precision compared with the ground truth is selected as the refined result so that the best performance is obtained from these schemes. For the proposed scheme, the CNN results are segmented into  $K$  regions, and refined by measuring the cost.

**Table 2.** Objective evaluation results for prostate segmentation.

Methods	Precision	Recall	Dice score
CNN-based scheme	0.62	0.96	0.74
Proposed scheme	0.78	0.81	0.78
CNN+Bias-correction	0.70	0.64	0.65
CNN+Nonparametric	0.70	0.65	0.65

For the performance evaluation, the precision, recall, and dice score are measured with 58 prostate MR images,  $320 \times 320$ , in the test set. As shown in Table 2, it is observable that the precision and dice score by the proposed scheme are the highest score in the compared schemes. In contrast, the recall is much lower than that of CNN-based scheme. The precision by LS-based schemes are higher than that of the CNN result while the recall score is the lowest. For visual comparison, the prostate segmentation results are shown in Figures 2, 3, and 4. The red and green lines indicate the ground truth and segmented result, respectively. As shown in the figures, the results of the CNN-based approach include most prostate and some non-prostate areas. The contours of the proposed method are much closer to the ground truth than those of the compared approaches. Therefore, the CNN and TD-based segmentation scheme can detect and segment the object of interest precisely.

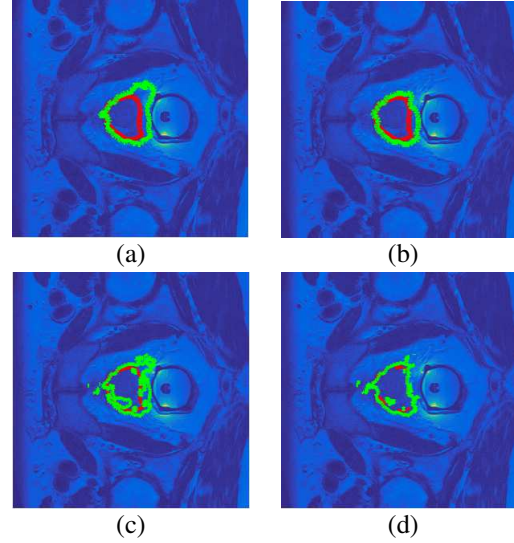


**Fig. 2.** Prostate segmentation performance comparison for a MR image. From top to bottom: (a) result by CNN-based method (precision : 0.59), (b) by the proposed scheme (precision: 0.74), (c) refined by the bias-correction approach (precision: 0.61); and (d) refined by the nonparametric approach (precision: 0.74).

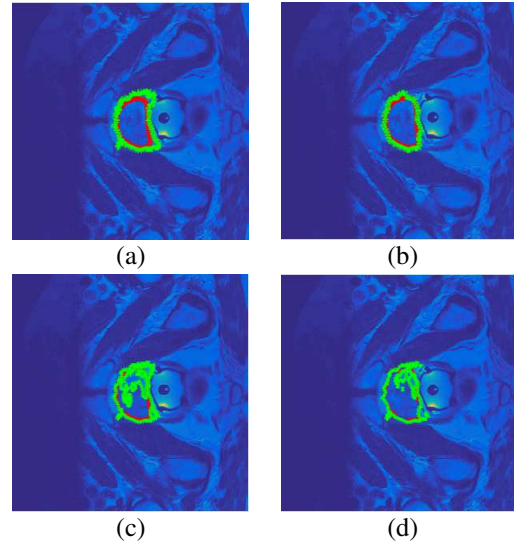


**Fig. 3.** Prostate segmentation performance comparison for a MR image. From top to bottom: (a) result by CNN-based method (precision : 0.74), (b) by the proposed scheme (precision : 0.92), (c) refined by the bias-correction approach (precision : 0.73); and (d) refined by the nonparametric approach (precision : 0.56).

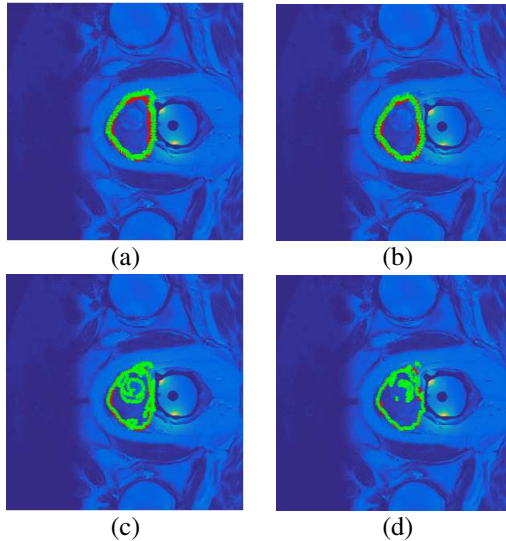


**Fig. 4.** Prostate segmentation performance comparison for a MR image. From top to bottom: (a) result by CNN-based method (precision : 0.86), (b) by the proposed scheme (precision : 0.97), (c) refined by the bias-correction approach (precision : 0.90); and (d) refined by the nonparametric approach (precision : 0.83).

#### 4. CONCLUSIONS

In this work, we proposed a CNN and TD-based prostate segmentation scheme. Specifically, the prostate region was detected by CNN-based method, and the result was adjusted by the connected-component labeling for removing the small regions. Thereafter, the CNN-results were improved by the TD-based segmentation and refinement methods. The performance evaluation was conducted by comparing the proposed method with a CNN-based scheme and the LS-based approaches used to refine the deep-learning results. Experimented results showed that the proposed scheme provided the highest score in the compared schemes. The contours of the proposed method were much closer to the ground truth than those by the compared approaches, and the performance of the CNN-based approach was improved by the proposed refinement scheme. Therefore, we believe that our proposed scheme can be a useful tool for prostate and organ segmentation in MR images.

#### 5. REFERENCES

- [1] Lequan Yu, Xin Yang, Hao Chen, Jing Qin, and Pheng-Ann Heng, "Volumetric convnets with mixed residual connections for automated prostate segmentation from 3d mr images," in *Thirty-First AAAI Conference on Artificial Intelligence (AAAI)*, 2017.
- [2] Chunming Li, Rui Huang, Zhaohua Ding, J Chris Gatenby, Dimitris N Metaxas, and John C Gore, "A level set method for image segmentation in the presence of intensity inhomogeneities with application to mri," *IEEE Transactions on Image Processing*, vol. 20, no. 7, pp. 2007–2016, 2011.
- [3] Marcelo Pereyra, Hadj Batatia, and Steve McLaughlin, "Exploiting information geometry to improve the convergence of nonparametric active contours," *IEEE Transactions on Image Processing*, vol. 24, no. 3, pp. 836–845, 2015.
- [4] Choong Sang Cho and Sangkeun Lee, "Low-complexity topological derivative-based segmentation," *IEEE Transactions on Image Processing*, vol. 24, no. 2, pp. 734–741, 2015.
- [5] Antonio André Novotny and Jan Sokołowski, *Topological derivatives in shape optimization*, Springer Science & Business Media, 2012.
- [6] Jonathan Long, Evan Shelhamer, and Trevor Darrell, "Fully convolutional networks for semantic segmentation," in *Proceedings of the IEEE Conference on Computer Vision and Pattern Recognition*, 2015, pp. 3431–3440.
- [7] Hyeonwoo Noh, Seunghoon Hong, and Bohyung Han, "Learning deconvolution network for semantic segmentation," in *Proceedings of the IEEE International Conference on Computer Vision*, 2015, pp. 1520–1528.
- [8] Tsung-Yi Lin, Michael Maire, Serge Belongie, James Hays, Pietro Perona, Deva Ramanan, Piotr Dollár, and C Lawrence Zitnick, "Microsoft coco: Common objects in context," in *European Conference on Computer Vision*. Springer, 2014, pp. 740–755.
- [9] M. Everingham, L. Van Gool, C. K. I. Williams, J. Winn, and A. Zisserman, "The PASCAL Visual Object Classes Challenge 2012 (VOC2012) Results," <http://www.pascal-network.org/challenges/VOC/voc2012/workshop/index.html>.
- [10] Oskar Maier, Bjoern H Menze, Janina von der Gabelntz, Levin Häni, Mattias P Heinrich, Matthias Liebrand, Stefan Winzeck, Abdul Basit, Paul Bentley, Liang Chen, et al., "Isles 2015-a public evaluation benchmark for ischemic stroke lesion segmentation from multispectral mri," *Medical image analysis*, vol. 35, pp. 250–269, 2017.
- [11] Geert Litjens, Robert Toth, Wendy van de Ven, Caroline Hoeks, Sjoerd Kerkstra, Bram van Ginneken, Graham Vincent, Gwenael Guillard, Neil Birbeck, Jindang Zhang, et al., "Evaluation of prostate segmentation algorithms for mri: the promise12 challenge," *Medical image analysis*, vol. 18, no. 2, pp. 359–373, 2014.